

# THE CHANDRA 3C SNAPSHOT SURVEY FOR SOURCES WITH $z < 0.3$

F. Massaro<sup>1</sup>, D. E. Harris<sup>1</sup>, D. Axon<sup>2</sup>, S. A. Baum<sup>3</sup>, A. Capetti<sup>4</sup>, M. Chiaberge<sup>5</sup>, R. Gilli<sup>6</sup>, G. Giovannini<sup>7</sup>, P. Grandi<sup>8</sup>, F. D. Macchetto<sup>5</sup>, C. P. O'Dea<sup>2</sup>, G. Risaliti<sup>9</sup>, W. Sparks<sup>5</sup>.



<sup>1</sup> Harvard, Smithsonian Astrophysical Observatory, Cambridge, MA, <sup>2</sup> Dept of Physics, Rochester Institute of Technology, Rochester, NY

<sup>3</sup> Carlson Center for Imaging Science, Rochester, NY

<sup>4</sup> INAF - Osservatorio Astronomico di Torino, Italy, <sup>5</sup> Space Telescope Science Institute, Baltimore, MD

<sup>6</sup> INAF - Osservatorio Astronomico di Bologna, Italy <sup>7</sup> INAF - Istituto di Radioastronomia di Bologna, Italy

<sup>8</sup> INAF-IASF - Istituto di Astrofisica Spaziale e fisica cosmica di Bologna, Italy <sup>9</sup> INAF - Osservatorio Astronomico di Arcetri, Italy



## 1 Introduction

The 3CR catalogue is the best studied sample of radio-loud AGNs in existence. It spans a wide range in redshift and in radio power. During the last few years a snapshot survey of 3CR sources using the Hubble Space Telescope has been performed and it approaches the completeness of the catalog for redshift  $z < 0.3$ . Radio maps are readily obtained from the VLA and MERLIN archives as well as from colleagues. The Chandra 3C Snapshot Survey, started in AO9, has the goal of completing the sample with X-ray data. The use of Chandra is required because it is the only X-ray facility with an angular resolution comparable to the HST and radio data and sufficient to resolve the radio components. 25 of the 30 targets in the first sample (AO Cycle 9) have already been observed as of 1 May 2008. The results of preliminary X-ray analyses, in comparison with data available at other wavelengths, are given here. The best examples of the detection of nuclear absorption and of extended structures (diffuse circumnuclear emission, jets, and hotspots) are here reported, and in these cases a comparison with VLA radio maps and HST images (IR and optical) is also shown. For the numerical results we used cgs units, unless stated otherwise. We assume a flat cosmology with  $H_0 = 72$  km/(s Mpc),  $\Omega_M = 0.27$  and  $\Omega_\Lambda = 0.73$  (see Spergel et al., 2007).

## 2 Nuclei

The X-ray nuclear emission has been detected in all cases with the exceptions of 3C 135 and 3C 315. We report the flux maps derived in the three X-ray bands (soft: 0.2-1.0 keV, medium: 1.0-2.0 keV and hard: 2.0-7.0 keV) for 3C 197.1, classified as BLRG, and 3C 76.1 (FR I radiogalaxy) (see Fig. 1 and Fig. 2).

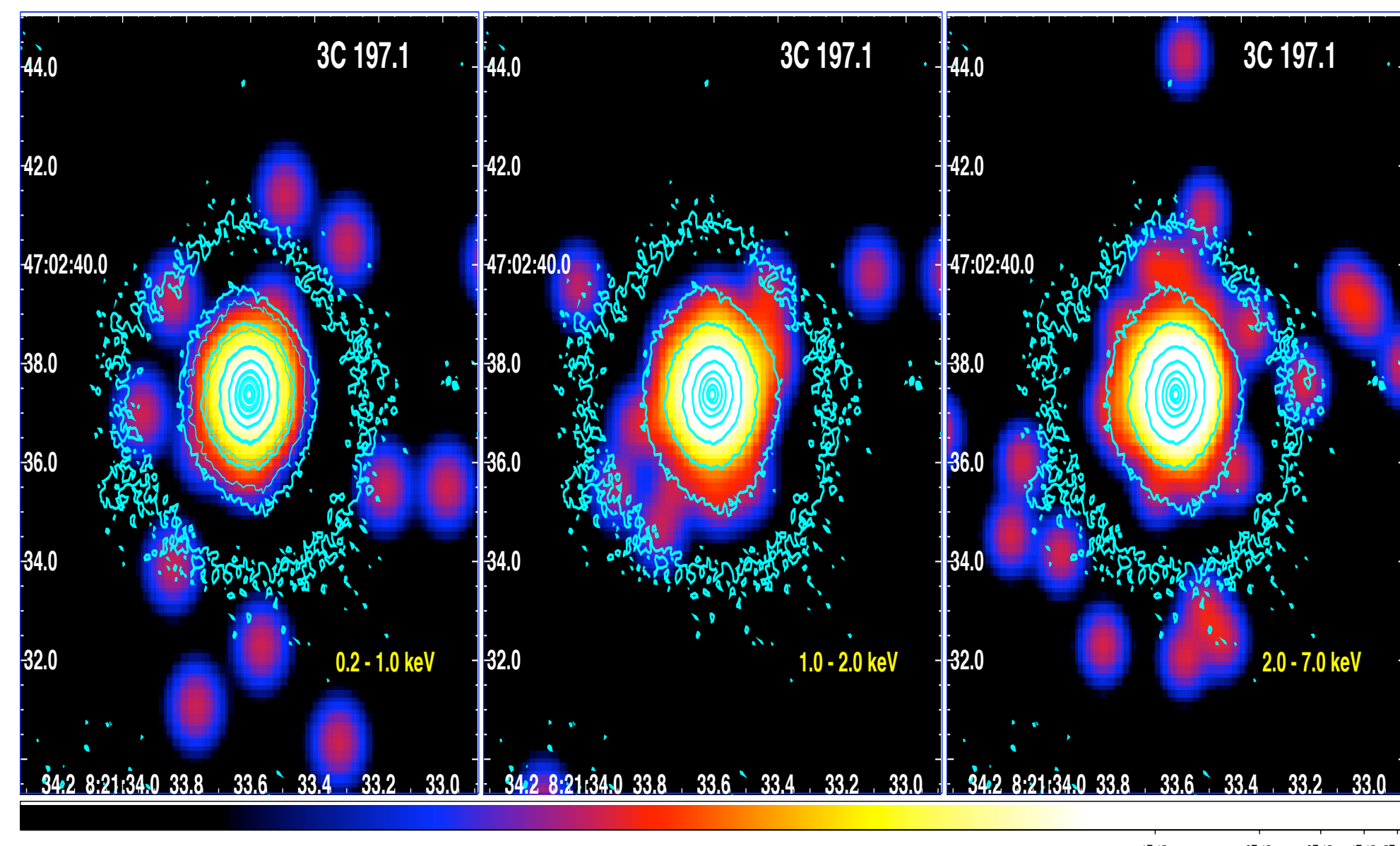


**Figure 1:** The X-ray image of 3C 197.1 in three different bands: soft (0.2 – 1.0 keV) (left panel), medium (1.0 – 2.0 keV) (middle panel) and hard (2.0 – 7.0 keV) (right panel). HST IR contours are also reported (cyan). The nuclear emission is detectable in all bands.

Intriguingly, the nucleus of 3C 76.1 is not detected below 1.0 keV, while that of 3C 197.1 is bright in the three different bands. The nucleus of 3C 76.1 is the faintest nucleus detected in our sample (i.e. 50 counts). The fact that we do not detect it at low frequencies could be due to absorption (from e.g. the moderately high Galactic column density,  $N_H \sim 9.5 \times 10^{20}$ , or from intrinsic absorption). An alternative scenario is that the faint nuclear emission we detect in this source is intrinsically hard. With the present data it is extremely difficult to discriminate between the possible scenarios. Our X-ray observations have the same exposure of about 8 ksec.

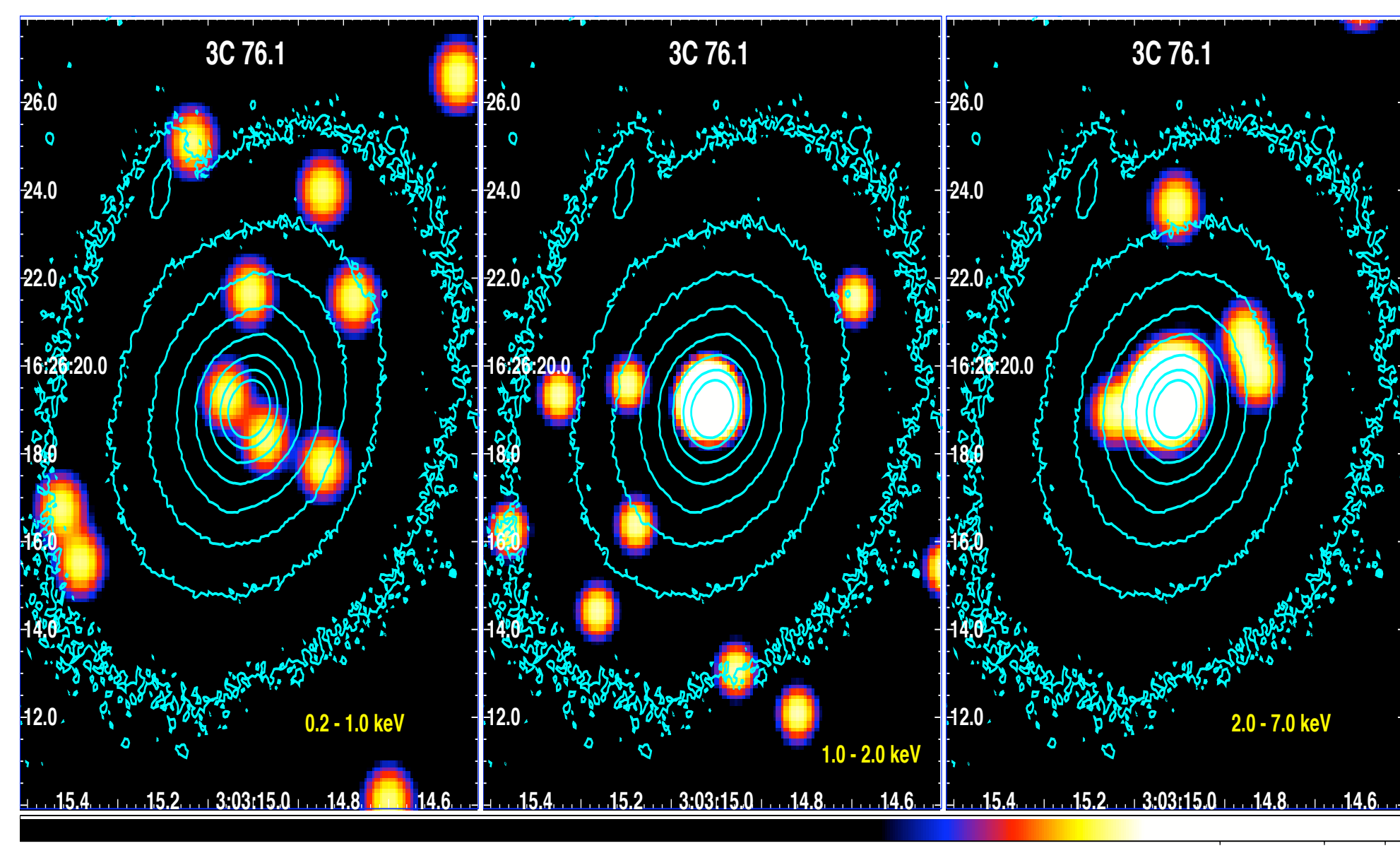


**Figure 2:** The X-ray image of 3C 76.1 in three different bands: soft (0.2 – 1.0 keV) (left panel), medium (1.0 – 2.0 keV) (middle panel) and hard (2.0 – 7.0 keV) (right panel). HST IR contours are also reported (cyan). There is no detection of nuclear emission in the soft band, while in the medium and in the hard it is detectable.

## 3 Diffuse emission

The case of 3C 332.0 ( $z=0.15$ ) represents the best example of extranuclear diffuse X-rays emission, and it is the most bright source in our sample. The X-ray diffuse emission, around the nucleus of 3C 332.0 extends to about  $7.5''$  (19.5 kpc), more than the Chandra PSF. The compact radio core of 3C 332.0 corresponds to a circular region with radius  $\leq 2.5''$  (6.5 kpc) (black contours in Fig. 3). The X-ray flux evaluated for the annular region in Fig. 3 in the 0.2-7.0 keV is  $1.62 \times 10^{-13}$  erg cm<sup>-2</sup> s<sup>-1</sup>.

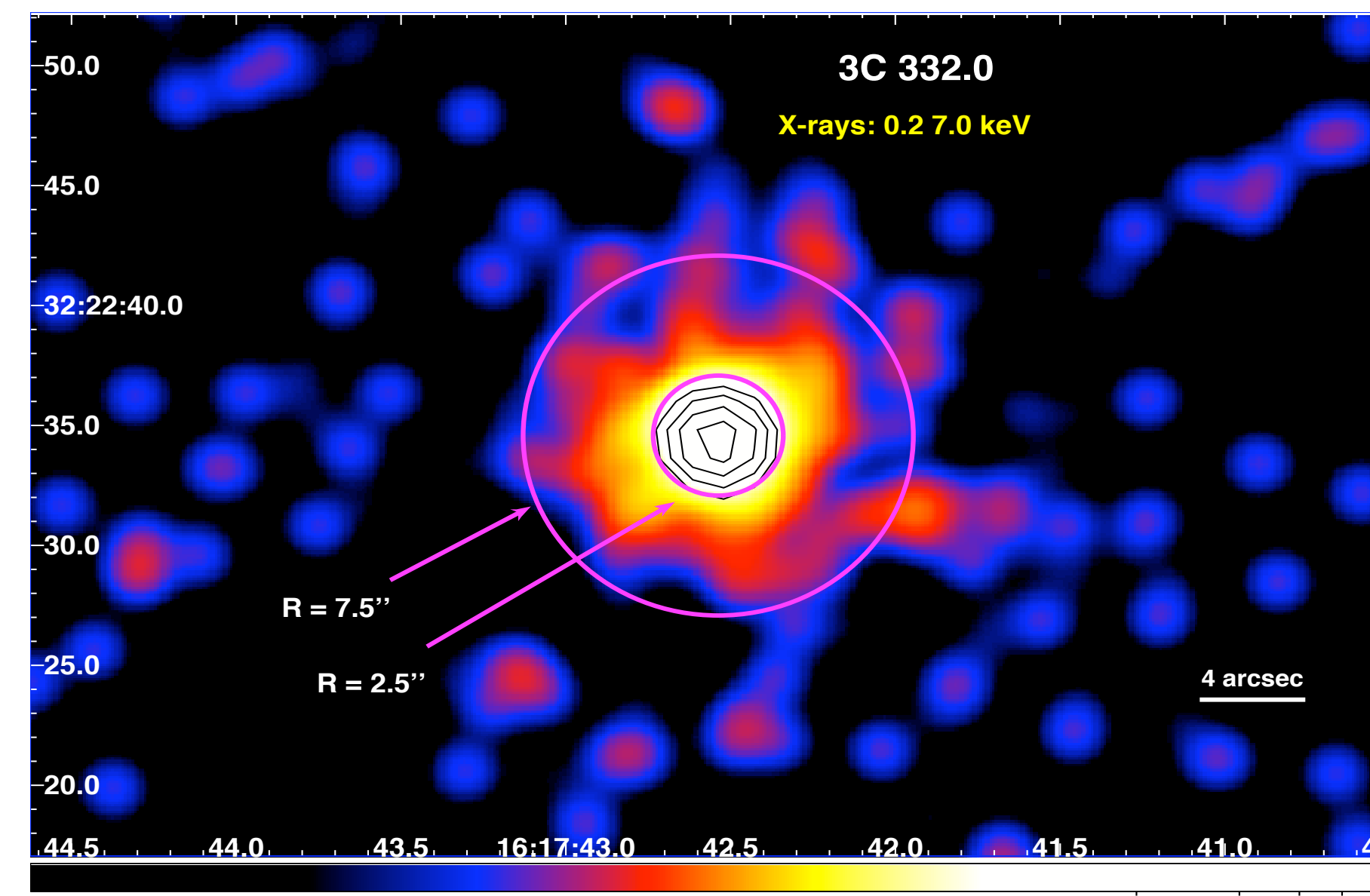


**Figure 3:** The X-ray image of 3C 332.0 with radio contours (black) to show the diffuse emission around the radio core.

## 4 Jets

The source 3C 17 represents the best example in our sample of an X-ray jet detection. The VLA radio map shows a bent jet (Morganti et al. 1999) in the southeast region (see Fig. 4). An X-ray counterpart for two radio knots has been found. The first knot lies at about  $3.7''$  (12.8 kpc) from the nucleus while the other detected knot is about  $11.3''$  (39.5 kpc) away. An optical counterpart has been detected for both knots Fig. 4 reports the HST image with X-rays (Chandra) and radio (VLA) contours.

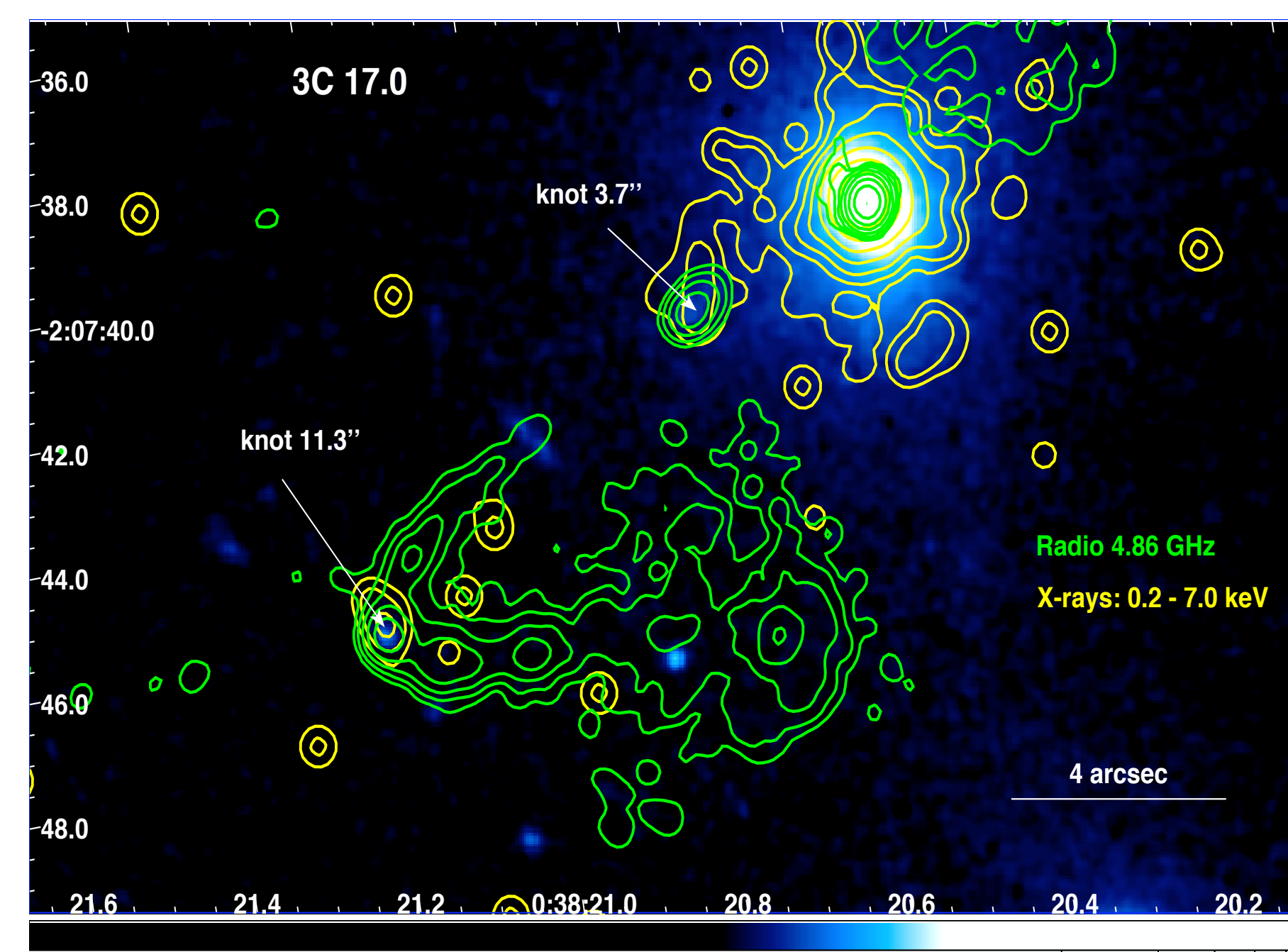


**Figure 4:** HST optical image of 3C 17. The radio contours are green while the X-ray are reported in yellow. The optical and X-ray counterparts are seen for both knots of the radio jet.

The spectrum of both knots in the 3C 17 jet is reported in Fig. 5. Optical to UV data are derived on using HST images. No IR emission is found for the knot  $11.3''$  because it is outside of the NICMOS camera (see Massaro et al. 2008 for details).

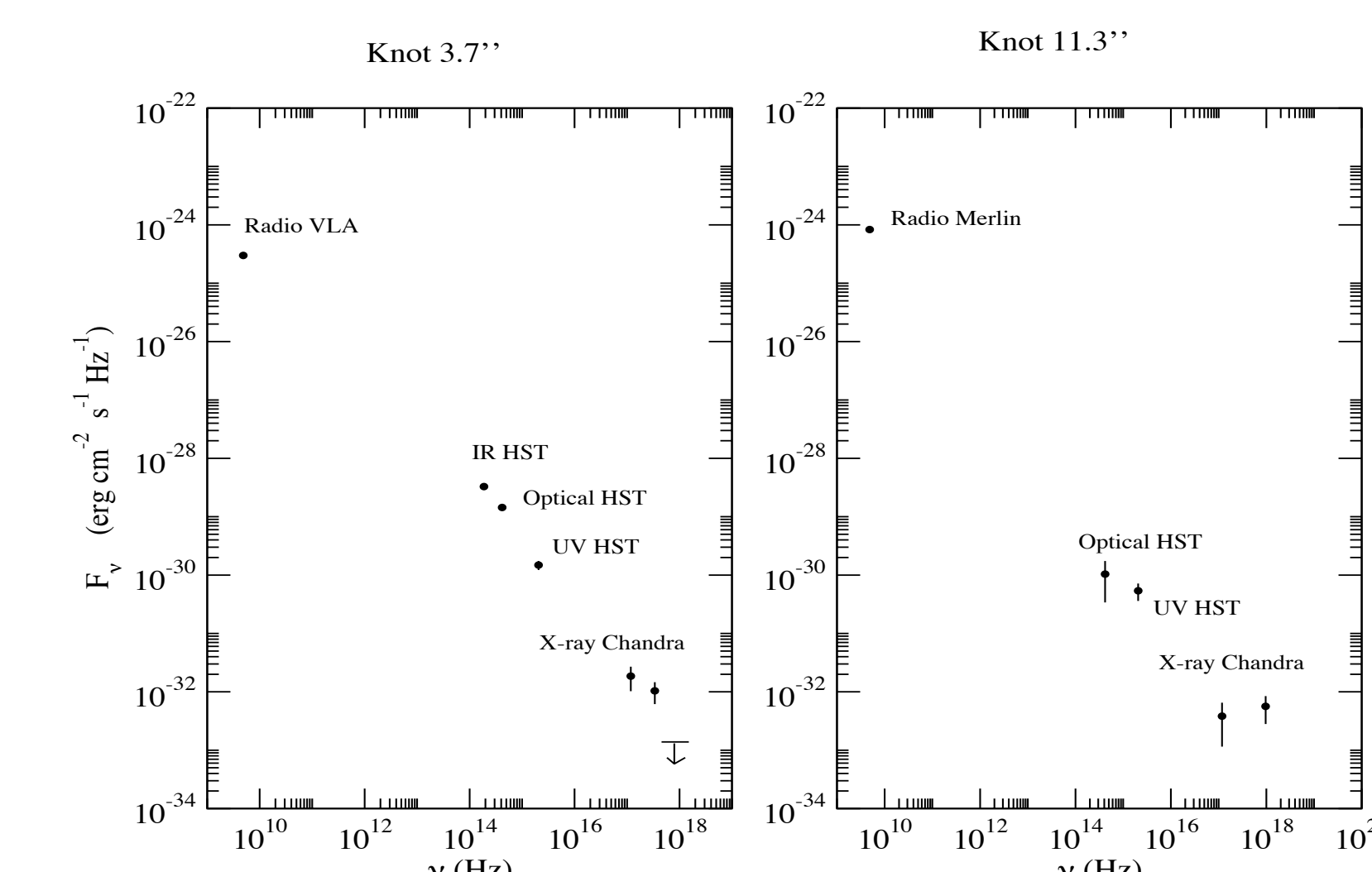


**Figure 5:** The spectrum of both knots in the radio jet of 3C 17, derived combining VLA, HST and Chandra data.

## 5 Hotspots

The detections of the X-ray emission associated to the SE hotspot of 3C 105 is shown in Fig. 6. The flux measured in the X-ray band between 0.2 – 7.0 keV is  $1.97 \times 10^{-14}$  erg cm<sup>-2</sup> s<sup>-1</sup>. Its distance corresponds to about 0.274 Mpc, projected.

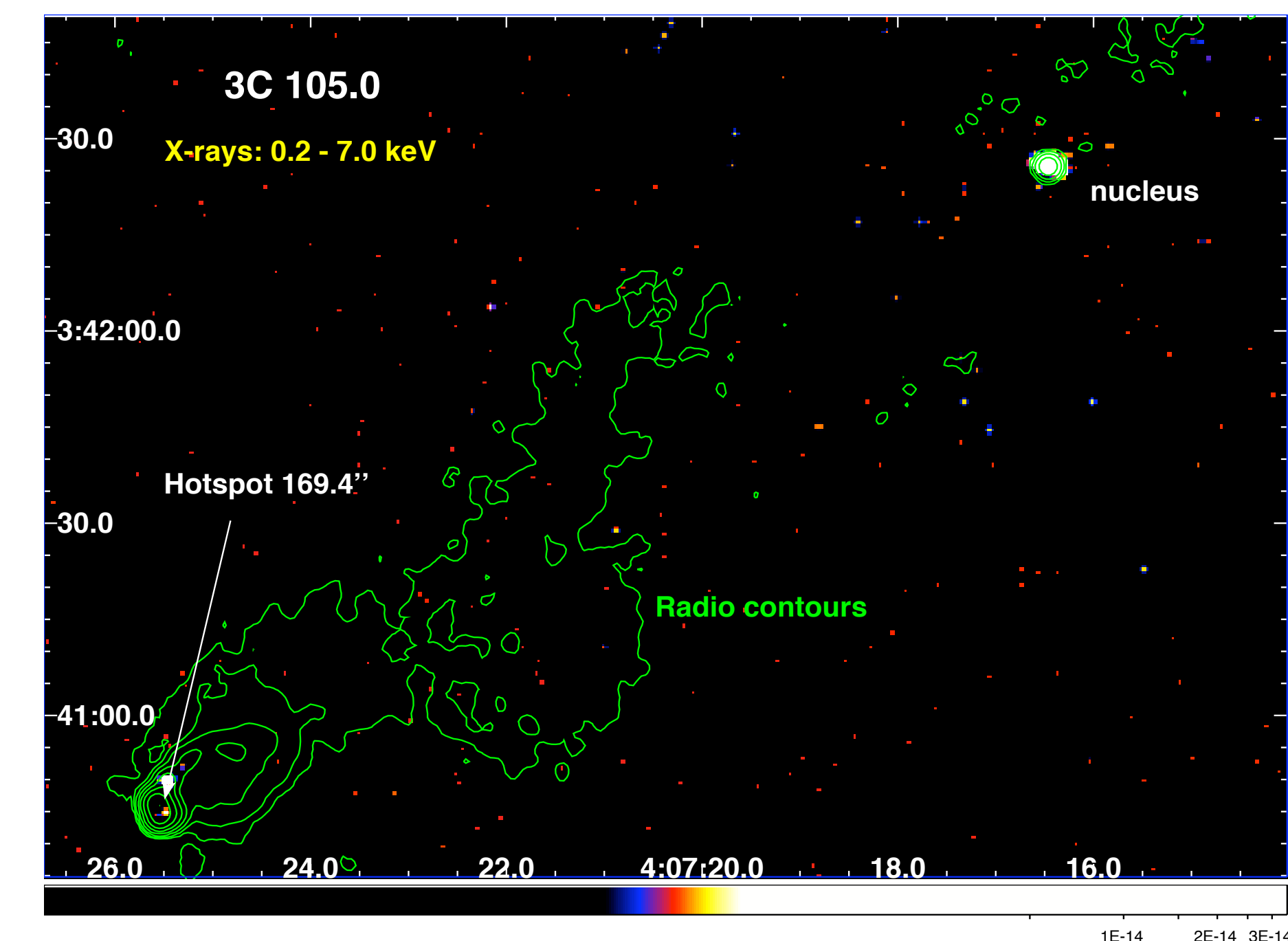


**Figure 6:** X-ray image of 3C 105. The overlaid green contours refer to the radio emission. Here, the radio hotspot at  $169.4''$  from the nucleus shows an X-ray counterpart with at least two separate components.

The X-ray emission detected for the hotspot E  $4.5''$  (16.6 kpc) is equal to  $4.28 \times 10^{-15}$  erg cm<sup>-2</sup> s<sup>-1</sup> in the 0.2 – 7.0 keV. Its emission is mostly in the soft X-rays between 0.2 - 2.0 keV. In Fig. 7 and Fig. 8 the radio and X-ray contours are overlaid to the HST images of 3C 171.0 at 5.484 nm and 5.007 nm [O III].

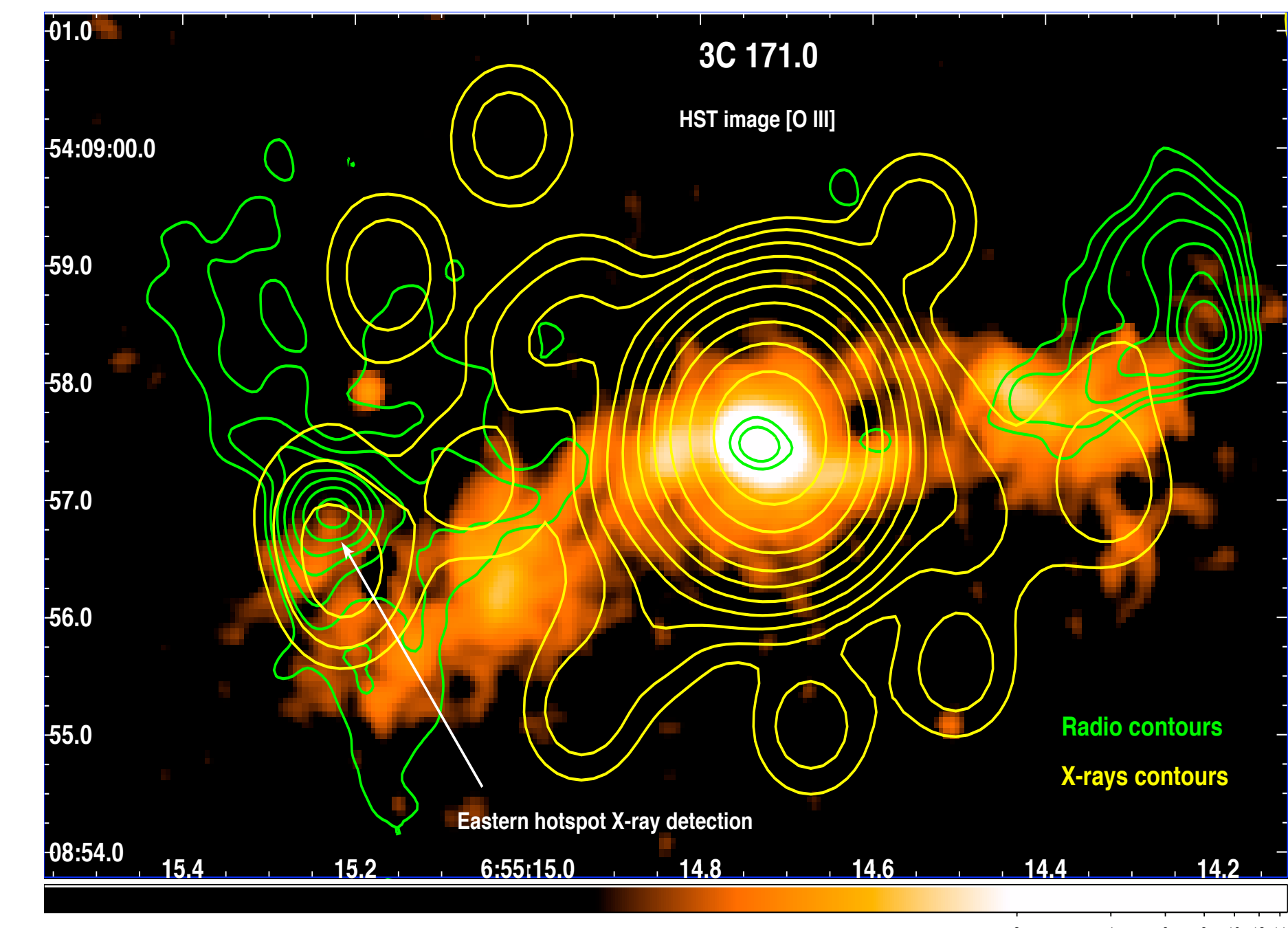


**Figure 7:** HST optical image of the [O III] emission line at 5.007 nm with radio (green) and X-ray (yellow) contours overlaid (see Tilak et al. 2005).

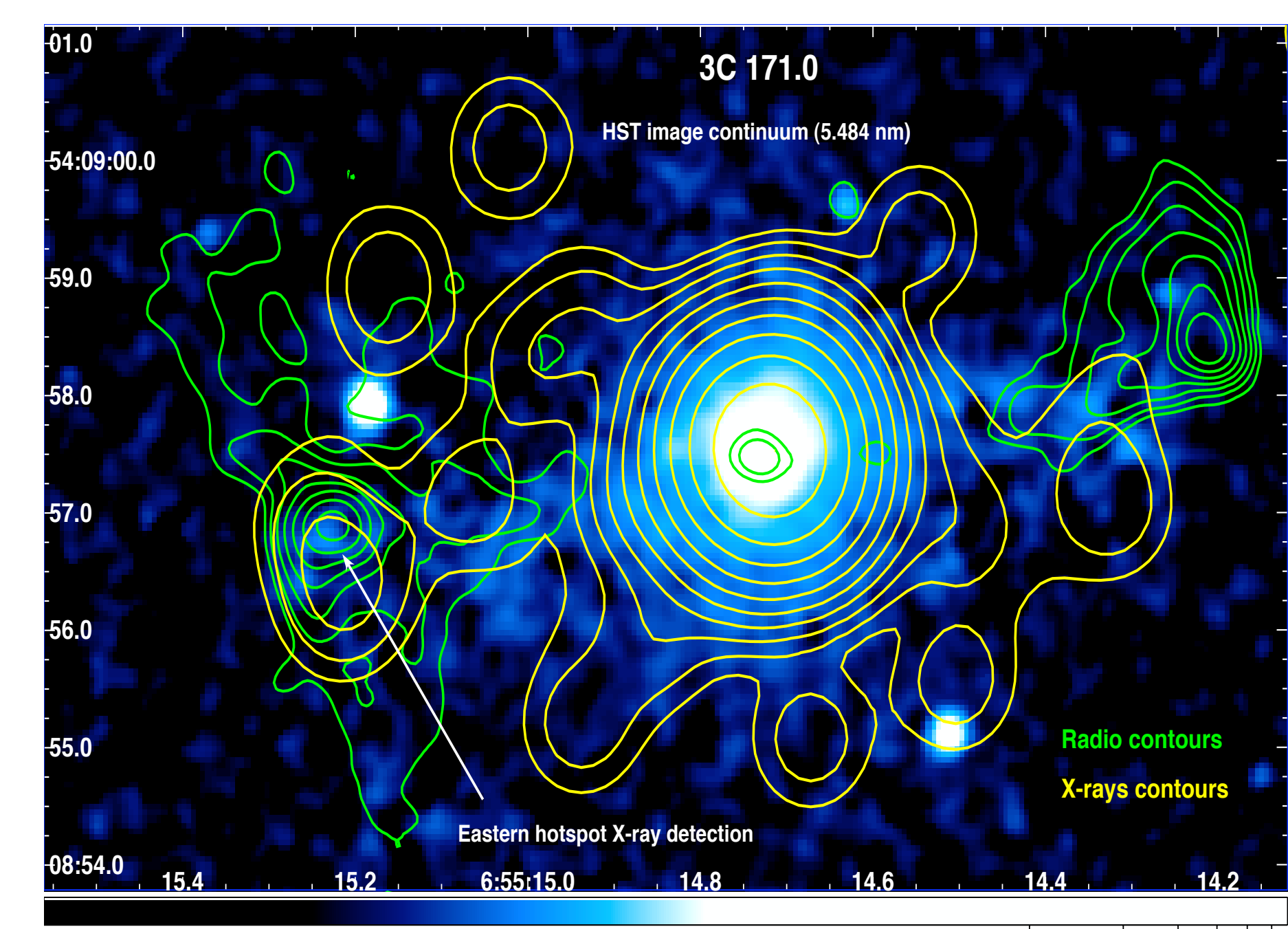


**Figure 8:** HST optical image of the continuum emission at 5.484 nm with radio (green) and X-ray (yellow) contours overlaid (see Tilak et al. 2005).

**Acknowledgments:** We thank A. Siemiginowska and J. McDowell for their help in the use of the CIAO data reduction analysis software. We are grateful to R. Morganti and M. J. Hardcastle for the archival radio maps. We also thank A. Tilak for the HST images of 3C 171.0. This research has made use of the NASA/IPAC Extragalactic Database (NED) which is operated by the Jet Propulsion Laboratory, California Institute of Technology, under contract with the National Aeronautics and Space Administration. This work is supported by NASA-GRANT G08-9114A.